A Phenomenological Model of the Synapse Between the Inner Hair Cell and Auditory Nerve: Implications of Limited Neurotransmitter Release Sites

Ian C. Bruce[1], Yousof Erfani[1] and Muhammad S. A. Zilany[2]

[1]Department of Electrical & Computer Engineering, McMaster University, Hamilton, ON, Canada

[2]Department of Computer Engineering, University of Hail, Hail, Saudi Arabia

Abstract

The auditory-periphery model of Zilany et al. (2014, 2009) introduced fractional Gaussian noise and power-law adaptation into a description of the synapse between the inner hair cell and auditory nerve fiber (ANF) to produce non-Poissonian fluctuations in the spike rate. However, the spike-generation is only driven by a single synaptic release process with instantaneous replenishment, consistent with a large number of release sites. Relative refractoriness is implemented with two time constants of 1 and 12.5 ms, which give an accurate distribution of inter-spike intervals (ISIs), but the statistics of successive ISIs are independent. In contrast, Peterson and colleagues have argued that the synapse may have a limited number of release sites ($\sim$ 4) with relatively long average replenishment times ($\sim$ 16 ms), giving rise to the non-independent successive ISI statistic observed in ANFs (Peterson and Heil, 2016; Peterson et al., 2014). We investigated how the approach of Peterson and colleagues could be incorporated into the synapse and spike-generation model of Zilany and colleagues. We modified the spike-generation description to have four identical parallel synaptic release processes, each with a quarter of the total desired release rate before refractoriness and a 16-ms average replenishment time, along with a separate mechanism for implementing the refractoriness of the ANF. Because of the inclusion of the 16-ms average replenishment time, only a single, short time constant is needed for the relative refractoriness. Preliminary simulations indicate that this modified model generates physiologically-realistic successive ISI statistics and fluctuations in spike-rate over time, which is important in accurately describing the spiking statistics that set the physiological limits for the neural encoding of sounds.

I. INTRODUCTION

- Figure 1 illustrates the ribbon synapse of the inner hair cell (IHC) to auditory nerve fiber (ANF).

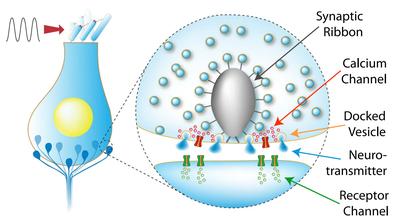

Figure 1: Illustration of the inner hair cell (IHC) to auditory nerve fiber (ANF) synapse. Note that there may only be a limited number of vesicle docking sites from which neurotransmitter can be release across the synaptic cleft. After exocytosis of a vesicle, it may take some time for a new vesicle to be transported from the synaptic ribbon to the empty docking site. Adapted with permission from `http://www.inmfrance.com/inm/fr/audition/90-lar-determinants-of-hair-cell-exocytosis`.

- As highlighted by Peterson et al. (2014) and Peterson and Heil (2016), the number of vesicle docking sites at each ribbon synapse and the rate at which redocking occurs after synaptic release has significant implications:

Large number of docking sites + Rapid redocking $\longrightarrow$ **Poisson release count statistics/ Independent exponential inter-release distributions**

Small number of docking sites + Slow redocking $\longrightarrow$ **Non-Poisson release count statistics/ Correlated gamma-like inter-release distributions**

II. MODEL STRUCTURE AND COMPUTATIONAL IMPLEMENTATION

- Peterson and Heil (2016) proposed a synapse model to describe the spontaneous activity of ANFs.
- In this study, their model is generalized to the case of acoustically-driven activity in addition to spontaneous activity and incorporated in to the auditory-periphery model of Zilany et al. (2014, 2009). The old and new synapse model structures are compared in Fig. 2.

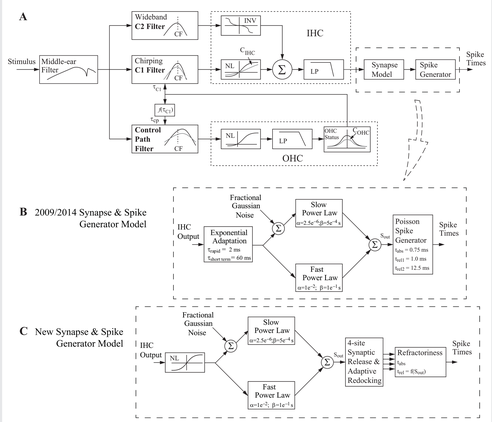

Figure 2: **A** Schematic of the model of the mammalian auditory periphery from Zilany et al. (2014, 2009). **B** IHC-ANF synapse model structure from the 2009/2014 version of the model. **C** Proposed new structure of the synapse model. Panels A & B adapted with permission from Zilany et al. (2009).

- The new model considers the case of 4 synaptic vesicle docking sites for exocytosis, as was found by Peterson et al. (2014) and Peterson and Heil (2016) to best explain the statistics for spontaneous activity in ANFs.
- Peterson et al. (2014) and Peterson and Heil (2016) proposed a fixed mean redocking (replenishment) time in the range 13.5–16 ms.
- This fixed mean redocking time can produce the rapid ($\sim$ 2 ms) exponential adaptation implemented previously in the auditory-periphery model by the Westerman and Smith (1988) exponential adaptation model (see Fig. 2B), but not the short-term ($\sim$ 60 ms) adaptation component.
- To produce short-term adaptation (with a time constant of $\sim$ 60 ms) as well in the new synapse model, an adaptive mean redocking time was implemented according to the dynamics:

$$\tau_{\mathrm{rd}}[n+1] = \begin{cases} \tau_{\mathrm{rd}}[n] + 0.4\times10^{-3}\cdot N_{\mathrm{rd}}[n], & \text{if } N_{\mathrm{rd}}[n] > 0, \\ \tau_{\mathrm{rd}}[n] + \frac{14\times10^{-3}-\tau_{\mathrm{rd}}[n]}{60\times10^{-3}}\Delta t, & \text{if } N_{\mathrm{rd}}[n] = 0, \end{cases} \tag{1}$$

where $\tau_{\mathrm{rd}}[n]$ has units of seconds, $N_{\mathrm{rd}}[n]$ is the number of synaptic redocking events that have occurred during time step n, which has a duration of Δt seconds, and τ_{rd} is initialized to a value of 13.6×10^{-3}+$0.02\times10^{-3}\cdot$ spont seconds, where spont is the desired spont rate (in units of spikes/s) of the ANF before redocking and refractoriness are considered.
- The adaptation in the mean redocking time can be explained in terms of an increase occurring after a synaptic redocking event because the vesicle that has docked will need to be replaced at its previous position on the synaptic ribbon by a more distant vesicles, and a decay back toward the resting value if no redocking events occur.
- This adaptive redocking mechanism allows for the removal of the Westerman and Smith (1988) model from its previous location before the power-law adaptation (PLA) model, replaced with a gently-saturating nonlinearity (compare panels B and C of Fig. 2).
- For the j^{th} synaptic release site, the time interval $T_{\mathrm{rd},i,j}$ from the i^{th} synaptic release to a vesicle redocking is modeled as an exponentially-distributed random number with mean $\tau_{\mathrm{rd}}[n]$ where n corresponds to the time step of the i^{th} release, and the time from that redocking to the next synaptic release is computed via numerical integration according to:

$$\int_{t_{i,j}+T_{\mathrm{rd},i,j}}^{t_{i+1,j}} \frac{S_{\mathrm{out}}(t)}{4}\,\mathrm{d}t \geq e_{i,j}, \tag{2}$$

where $t_{i,j}$ is the time of the j^{th} synaptic release for the j^{th} site, $t_{i+1,j}$ is the time of the next synaptic release on that site, $S_{\mathrm{out}}(t)$ is the output of the PLA model and corresponds to the desired total synaptic release rate (in spikes/s) across the 4 sites before considering the effects of redocking, and $e_{i,j}$ is an exponentially-distributed random number with a mean of 1.
- Following Peterson et al. (2014) and Peterson and Heil (2016), synaptic release from any of the 4 sites in time step n can generate an action potential in the model ANF as long as it is not in a refractory state.
- Peterson et al. (2014) and Peterson and Heil (2016) used a fixed absolute refractory period of 0.75 ms and an exponentially-distributed relative refractory period with a mean duration of 0.75 ms.
- However, the data of Miller et al. (2001) indicate that ANFs may each have different values for their absolute and relative refractory periods. Furthermore, the data of Li and Young (1993) indicate that the effective relative refractory period may be shorter for higher synaptic release rates, which would be consistent with multiple postsynaptic potentials being more likely to sum temporally to reach the elevated threshold potential observed during relative refractoriness.
- Thus, in the new model t_{abs} can take a range of values based on the distribution from Miller et al. (2001). Likewise, the baseline mean relative refractory period $\hat{t}_{\mathrm{rel}}$ can take a range of values based on the distribution from Miller et al. (2001), and the mean relative refractory period for time step n is computed according to:

$$t_{\mathrm{rel}}[n] = \min\left\{\frac{100\,\hat{t}_{\mathrm{rel}}}{S_{\mathrm{out}}[n]}, 2\,\hat{t}_{\mathrm{rel}}\right\}. \tag{3}$$

- Peterson and Heil (2016) argued that the standard deviation of the fractional Gaussian noise (fGn) in the Zilany et al. (2014, 2009) model (see panels B and C of Fig. 2) should be reduced substantially. In this study we found it sufficient to reduce the fGn std to a value of 1 for low-spont fibers, 10 for medium-spont fibers and spont/2 for high-spont fibers.

III. ANALYTICAL ESTIMATES OF MEAN AND VARIANCE IN SPIKE RATE

- Consider the case where S_{out}, τ_{rd} and t_{rel} are constant.
- The distribution of intervals between synaptic release events at the j^{th} docking site T_j can be obtained by convolving the exponential distributions for the redocking time and the release time to obtain:

$$f(T_j) = \frac{S_{\mathrm{out}}}{S_{\mathrm{out}}\tau_{\mathrm{rd}} - 4}\left\{\mathrm{e}^{-T_j/\tau_{\mathrm{rd}}} - \mathrm{e}^{-S_{\mathrm{out}}T_j/4}\right\}, \quad \text{for } T_j \geq 0. \tag{4}$$

- From Cox and Smith (1954), the superposition of N renewal processes described by (4) gives a distribution of intervals between release events T that can be found via:

$$f(T) = -\frac{\mathrm{d}}{\mathrm{d}T}\left\{F_c(T)\left[\int_T^\infty \frac{F_c(x)}{\mathrm{E}[T_j]}\mathrm{d}x\right]^{N-1}\right\}, \tag{5}$$

where $F_c(T)$ is the complementary cumulative distribution function corresponding to the single-site distribution (4) and $\mathrm{E}[T_j]$ is the mean time between release events at a single site.
- The effects of refractoriness on the distribution of inter-spike intervals (ISIs) can be obtained by convolving the distribution from (5) with the refractory period distribution:

$$p(t) = \mathrm{e}^{-(t-t_{\mathrm{abs}})/t_{\mathrm{rel}}}, \quad \text{for } t \geq t_{\mathrm{abs}}. \tag{6}$$

- Also from Cox and Smith (1954), the mean and variance of the spike rate can then be obtained via:

$$\mathrm{E}[\mathrm{rate}] = \frac{1}{\mathrm{E}[\mathrm{ISI}]}; \qquad \mathrm{var}[\mathrm{rate}] = \frac{\mathrm{var}[\mathrm{ISI}]}{\mathrm{E}[\mathrm{ISI}]^3}. \tag{7}$$

IV. RESULTS

- Overall, the simulation results from this study showed equal or improved accuracy in predicting published ANF data compared to the results of Zilany et al. (2014, 2009). The results shown here are for cases where there were substantial improvements achieved by the new model.
- Analytical estimates of the mean and variance in spike rate obtained using the method given in Section III are shown in Fig. 3.

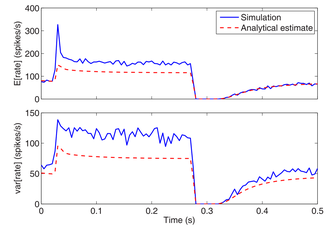

Figure 3: Simulation results and analytical estimates of the mean (top panel) and variance (bottom panel) in the spike rate for a 250-ms long stimulus (t = 25 to 275 ms).

- The Fano factor $F(T) = \mathrm{var}[N(T)]/\mathrm{E}[N(T)]$ where $N(T)$ is the number of spikes in the time period T. Figure 4 compares the model Fano factor behavior to data from an example ANF.

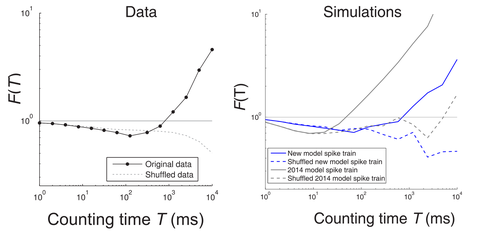

Figure 4: The Fano factor as a function of counting time for an example high-spont ANF (left panel) from Peterson et al. (2014) and for the 2014 and new synapse models (right panel).

- The serial interspike interval correlation coefficient (SIICC) measures the interdependence of N consecutive ISIs according to:

$$\rho = \frac{(N-2)^{-1}\sum_{i=1}^{N-1}(\mathrm{ISI}_i - \mathrm{E}[\mathrm{ISI}])(\mathrm{ISI}_{i+1} - \mathrm{E}[\mathrm{ISI}])}{(N-1)^{-1}\sum_{i=1}^{N}(\mathrm{ISI}_i - \mathrm{E}[\mathrm{ISI}])^2}. \tag{8}$$

- Figure 5 compares the model SIICC behavior to data from a population of ANFs.

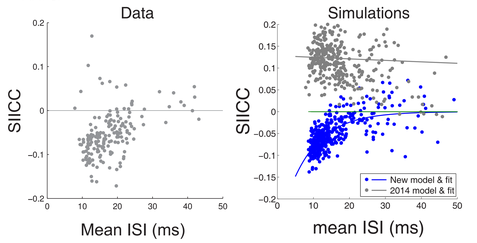

Figure 5: The serial interspike interval correlation coefficient (SIICC) as a function of mean ISI for a population of ANFs (left panel) from Peterson et al. (2014) and for the 2014 and new synapse models (right panel).

- In Figure 6, simulation results for estimates of the relative refractory period of individual ANFs are compared to published data.

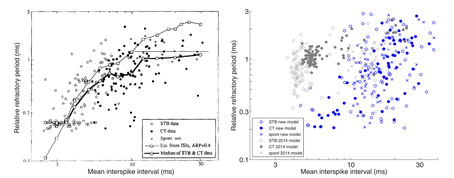

Figure 6: Relative refractory period estimates versus mean ISI for a population of ANFs (left panel) from Li and Young (1993) and simulation results (right panel) with the 2014 and new models for the cases of short tone burst (STB) or continuous tone (CT) stimulation or spontaneous activity.

- In Figures 7 and 8, simulation results for an ANF forward masking paradigm are compared to published data.

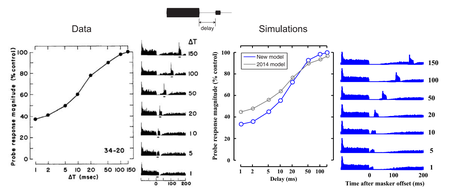

Figure 7: Physiological forward-masking data (left panels) for an example ANF from Harris and Dallos (1979) and simulation results (right panels) for the 2014 and new models. Masker tone at 30 dB above threshold and probe tone at 20 dB re. threshold.

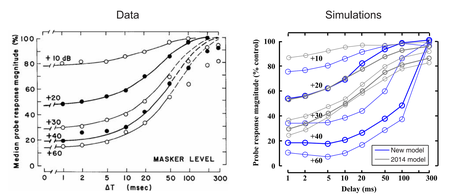

Figure 8: Median ANF forward-masking curves at a range of masker levels for a population of ANFs (left panel) from Harris and Dallos (1979) and simulation results (right panel) for the 2014 and new models. Probe tone at 20 dB re. threshold and masker level as labeled.

V. CONCLUSIONS

- Limiting the number of release sites in the IHC-ANF synapse model to 4 gives improved prediction of ANF spiking statistics.
- Using an adaptive mean redocking time, rather than the fixed values used by Peterson et al. (2014) and Peterson and Heil (2016), can explain the double-exponential adaptation previously obtained with the Westerman and Smith (1988) model placed before the power-law adaptation model and gives improved predictions of physiological forward masking in ANFs.

REFERENCES

Cox, D. R. and Smith, W. L. (1954). On the superposition of renewal processes. *Biometrika*, 41:91–99.

Harris, D. M. and Dallos, P. (1979). Forward masking of auditory nerve fiber responses. *J. Neurophysiol.*, 42(4):1083–1107.

Li, J. and Young, E. D. (1993). Discharge-rate dependence of refractory behavior of cat auditory-nerve fibers. *Hear. Res.*, 69(1):151–162.

Miller, C. A., Abbas, P. J., and Robinson, B. K. (2001). Response properties of the refractory auditory nerve fiber. *J. Assoc. Res. Otolaryngol.*, 2(3):216–232.

Peterson, A. J. and Heil, P. (2016). A revised model of synaptic release accounts for interspike-interval distributions, spike-count distributions, and non-renewal properties of spontaneous spike trains of auditory-nerve fibers. In *39th ARO Midwinter Meeting*, San Diego, CA.

Peterson, A. J., Irvine, D. R. F., and Heil, P. (2014). A model of synaptic vesicle-pool depletion and replenishment can account for the interspike interval distributions and nonrenewal properties of spontaneous spike trains of auditory-nerve fibers. *J. Neurosci.*, 34(45):15097–15109.

Westerman, L. A. and Smith, R. L. (1988). A diffusion model of the transient response of the cochlear inner hair cell synapse. *J. Acoust. Soc. Am.*, 83(6):2266–2276.

Zilany, M. S. A., Bruce, I. C., and Carney, L. H. (2014). Updated parameters and expanded simulation options for a model of the auditory periphery. *J. Acoust. Soc. Am.*, 135(1):283–286.

Zilany, M. S. A., Bruce, I. C., Nelson, P. C., and Carney, L. H. (2009). A phenomenological model of the synapse between the inner hair cell and auditory nerve: Long-term adaptation with power-law dynamics. *J. Acoust. Soc. Am.*, 126(5):2390–2412.

ibruce@ieee.org | erfaniy@mcmaster.ca | msazilany@gmail.com

Supported by NSERC, ACOA, and the Government of Newfoundland & Labrador